ChemPubSoc Europe

DOI: 10.1002/celc.201300195

Germanium-Based Electrode Materials for Lithium-Ion Batteries

Yang Liu,[a] Sulin Zhang,*[b] and Ting Zhu*[c]

Lithium-ion batteries (LIBs) with superior energy density, rate capability, and cyclability are critically needed for next-generation portable electronics and electric vehicles. Germanium (Ge) is a promising candidate material for the high-capacity anode of LIBs. Although the cost of Ge is the main barrier for its wide application in large-scale electrochemical energy storage, the electrochemical performance of Ge in LIBs is interesting from both scientific and engineering perspectives. Compared to silicon (Si), Ge has received much less attention, despite the relatively high electronic conductivity and high lithiation–delithiation rate in Ge. In this Concept, we review recent progress in the in situ electrochemical study of the lithiation and delithiation mechanisms in Ge nanowires and nanoparticles. Insights into the nanostructural evolution and mechanical degradation during electrochemical reactions are highlighted. Critical unresolved questions are raised and prospects for the future research of Ge-based electrodes are discussed.

1. Introduction

Advanced energy-storage systems are critically important for meeting the ever-increasing demand for applications from portable electronics to all-electric vehicles, and recently for applications in the grid for storing energy from fluctuating renewable sources, such as wind or solar energy. Lithium-ion batteries (LIBs) have received worldwide attention as a top performing energy-storage system. Currently, graphite is being used as the commercial anode material in LIBs. However, graphite has a relatively low theoretical capacity of 372 $mA\,h\,g^{-1}$, which significantly limits the fast-growing demand in energy storage. Other group-IV elements, such as Si, Ge, and Sn, are being considered as substitutes of graphite in LIBs because of their much higher theoretical capacities.[1] Among these candidate anode materials, Si is the most popular one and has been extensively studied. This is because Si possesses the highest theoretical capacity, 4200 $mA\,h\,g^{-1}$ for $Li_{22}Si_5$ at high temperature[2,3] or 3579 $mA\,h\,g^{-1}$ for $Li_{15}Si_4$ at room temperature,[4,5] which is about one order of magnitude higher than that of the graphite anode material.

Compared to Si, Ge has received much less attention, despite its high volumetric capacity (7366 $A\,h\,L^{-1}$ for $Li_{15}Ge_4$), second only to silicon (8334 $A\,h\,L^{-1}$ for $Li_{15}Si_4$), as well as its high gravimetric capacity (1384 $mA\,h\,g^{-1}$ for $Li_{15}Ge_4$).[1,6] Although Ge is more costly than Si, which could be the main reason for the lack of attention in the past, Ge has several outstanding features as a promising high-capacity anode material: 1) High electronic conductivity: since the bandgap of Ge (E_g = 0.66 eV at 300 K) is smaller than that of Si (E_g = 1.12 eV at 300 K),[7] Ge has a much higher intrinsic electronic conductivity than Si. 2) High lithium (Li) ion diffusivity: the diffusivity of the Li ion in Ge is about two orders of magnitude larger than that in Si at room temperature.[8,9] With these favorable transport properties, it is expected that Ge will have a better rate capability than Si. Fast transport of both electrons and Li ions is highly desired for achieving a high charging/discharging rate in LIBs.[8] Thus, a battery design that balances optimal energy and power densities could be achieved through Ge-based LIBs. With technical improvements to produce Ge, which is abundant in the Earth's crust, it is anticipated that the price of Ge could be reduced in the near future. In recent years, there has been a drastic increase in scientific research on Ge and Ge-based materials for applications in LIBs.[6,10–44]

A major drawback of high-capacity electrode materials, such as Si and Ge, is the huge volume change upon full lithiation/delithiation (about 281% for $Li_{15}Si_4$ and 246% for $Li_{15}Ge_4$),[45] which could result in pulverization of the electrode and delamination from the current collector, thereby leading to a significant capacity loss of the LIBs.[46–49] The large volume change is also believed to be responsible for damages in the solid electrolyte interphase (SEI), causing irreversible capacity loss. The severe mechanical degradation of both the anode and SEI prevents Si and Ge from commercialization. To address this issue, various types of nanostructures, such as nanowires, nanotubes, and nanoparticles, have been studied with encouraging improvement in capacity retention compared to their

[a] Dr. Y. Liu
Center for Integrated Nanotechnologies (CINT)
Sandia National Laboratories
Albuquerque, New Mexico 87185 (USA)

[b] Prof. S. Zhang
Department of Engineering Science and Mechanics
The Pennsylvania State University
University Park, PA 16802 (USA)
E-mail: suz10@psu.edu

[c] Prof. T. Zhu
Woodruff School of Mechanical Engineering
Georgia Institute of Technology
Atlanta, GA 30332 (USA)
E-mail: ting.zhu@me.gatech.edu

bulk counterparts. Such improvement has been attributed to the facile strain accommodation and the short diffusion path for electron and Li-ion transport in these nanostructured electrodes.[50–54]

After the seminal work by Chan et al. on Si nanowires as a novel anode material for LIBs,[47] a follow-up work was reported on Ge nanowires grown via the vapor–liquid–solid (VLS) method, and an initial discharge capacity of 1141 mA h g^{-1} was achieved at a rate of C/20.[10] Recent studies were also performed on other types of Ge nanostructures, such as nanotubes,[13] nanoparticles,[14,15,40] and thin films.[6,16] It is noteworthy that compared to solid nanowires, hollow nanotubes have the additional advantages of an even larger surface area to facilitate Li-ion transport, as well as the bidirectional accommodation (both inward and outward) of volume expansion. For example, Park et al. prepared ultra-long Ge nanotubes from core–shell Ge–Sb nanowires using the Kirkendall effect at 700 °C.[13] The Ge nanotubes exhibited an exceptionally high rate capability, up to 40 C (40 A g^{-1}), while maintaining a reversible capacity larger than 1000 mA h g^{-1} over 400 cycles. After 400 cycles, porous structures formed in the amorphous Ge nanotubes.

Besides engineering the geometry of Ge nanostructures, the alloying/integration of Ge with other elements, such as Si,[35,36,44] Sn,[33] Ti,[38] Cu,[34,37,41] and carbon (in forms of graphene,[26–29] carbon nanotubes,[23–25] and other carbon composites[17–22]), have also been investigated. These studies aimed to take advantage of each individual alloy constituent, as well as their collective effects, so as to optimize the anode performance. Song et al. developed Si/Ge double-layered nanotube array electrodes for LIBs and measured a capacity of 1746.1 mA h g^{-1} in the first discharge and 1544.6 mA h g^{-1} in the first charge. This value is larger than the theoretical capacity for pure Ge.[36] Also, the capacity retention at 3C rate is two times that reported for analogous homogeneous Si nanotubes. The high capacity and good rate capability are ascribed to the combination of Ge and Si to enhance the overall performance. Xue et al. used hybrid Ge/C core–shell nanoparticles with reduced graphene oxide as an anode material for LIBs. Their measurements showed an average columbic efficiency larger than 99% for up to 50 cycles after the second cycle and an enhanced capacity of 380 mA h g^{-1} after 50 cycles under a high current density of 3600 mA g^{-1}, compared with a capacity of 100 mA h g^{-1} for Ge/C nanoparticles under the same current and cycling conditions. The improved cycling performance and rate capability were attributed to the electronically conductive and elastic networks of the reduced graphene oxide, as well as the effective mechanical buffering of the carbon shell.[21] Yu et al. demonstrated that a 3D bicontinuous Au/amorphous Ge thin-film electrode fabricated by thermal evaporation can deliver a reversible capacity of up to 1200 mA h g^{-1} and have a capacity retention of 90% even after 100 cycles. This improved performance was attributed to the facile ion/electron transport in the network structure of the bicontinuous electrode and the ability of the 3D porous structure to accommodate large volume changes.[42]

2. In Situ TEM Electrochemistry

Although the battery performance can be significantly improved with nanostructured Ge-based materials, the fundamental mechanisms of the reaction, diffusion, microstructure evolution, and damage accumulation in electrodes during electrochemical cycling cannot be fully understood by ex situ coin cell testing. Recently, in situ transmission electron microscopy (TEM) electrochemistry has emerged as a powerful approach to reveal the dynamic processes of electrochemical reactions and mechanical degradations in electrodes at the nanoscale.[45,55] This novel method is capable of capturing the structural and phase evolution—as well as the changes in chemical composition—of nanostructured electrodes with a high resolution (down to the atomic scale) in real time.[48,56–76] Details of the in situ experimental setup can be found in recent reviews.[45,55] In this Concept, we highlight the recent study of lithiation/delithiation behaviors in Ge nanowires and nanoparticles by using the in situ TEM electrochemistry technique. New phenomena and understanding, including a two-step phase transformation (*c*-Ge → *a*-Li$_x$Ge → *c*-Li$_{15}$Ge$_4$), fast lithiation kinetics, isotropic swelling during lithiation, nanoporosity formation after delithiation, and a tough fracture behavior, are reviewed to provide mechanistic insights into the electrochemo-mechanical processes in Ge electrodes. Finally, open questions about Ge-based electrodes, as well as prospects for future research and applications, are discussed.

3. Mechanistic Insights into the Lithiation/Delithiation of Ge Electrodes

Figures 1 a–e show the typical microstructural evolution in a crystalline $<112>$-Ge nanowire during the first lithiation. The Li ions diffuse both along the surface and into the core along the radial direction. The resulting core–shell structure, with negligible tapering, indicates that the transport of Li ions on the nanowire surface is much faster than that in the bulk. Li alloys with crystalline Ge (*c*-Ge) to form amorphous Li$_x$Ge (*a*-Li$_x$Ge),[39] similar to the electrochemically driven solid-state amorphization process in Si.[77,78] Fast surface diffusion and solid-state amorphization were also observed in Si nanowires.[79,80] The magnified TEM image in Figure 1 i clearly shows the core–shell structure: an unlithiated *c*-Ge core is enclosed by a lithiated *a*-Li$_x$Ge shell with clear gray contrast. A thin surface layer of Li$_2$O is formed by lithiation of the surface native oxide. A lithiated *a*-Li$_x$Ge nanowire (Figure 1 d) is quickly crystallized, as evidenced from the crystal contrast shown in Figure 1 e and the electron diffraction pattern (EDP) in Figure 1 h. The EDPs shown in Figures 1 f–h verify the two-step phase transformation: *c*-Ge → *a*-Li$_x$Ge → *c*-Li$_{15}$Ge$_4$, which is similar to the first lithiation in crystalline Si.[79] During lithiation, the Li-rich (i.e. $x \sim 3.75$) and Li-poor (e.g. $x \sim 2.5$) phases of *a*-Li$_x$Ge could possibly be formed at different lithiation stages or coexist, similar to the lithiation of Si.[81,82] However, a phase boundary separating the Li-rich and Li-poor phases of Li$_x$Ge was not observed by our in situ TEM studies, probably because the transformation from the Li-poor to Li-rich phase occurred too

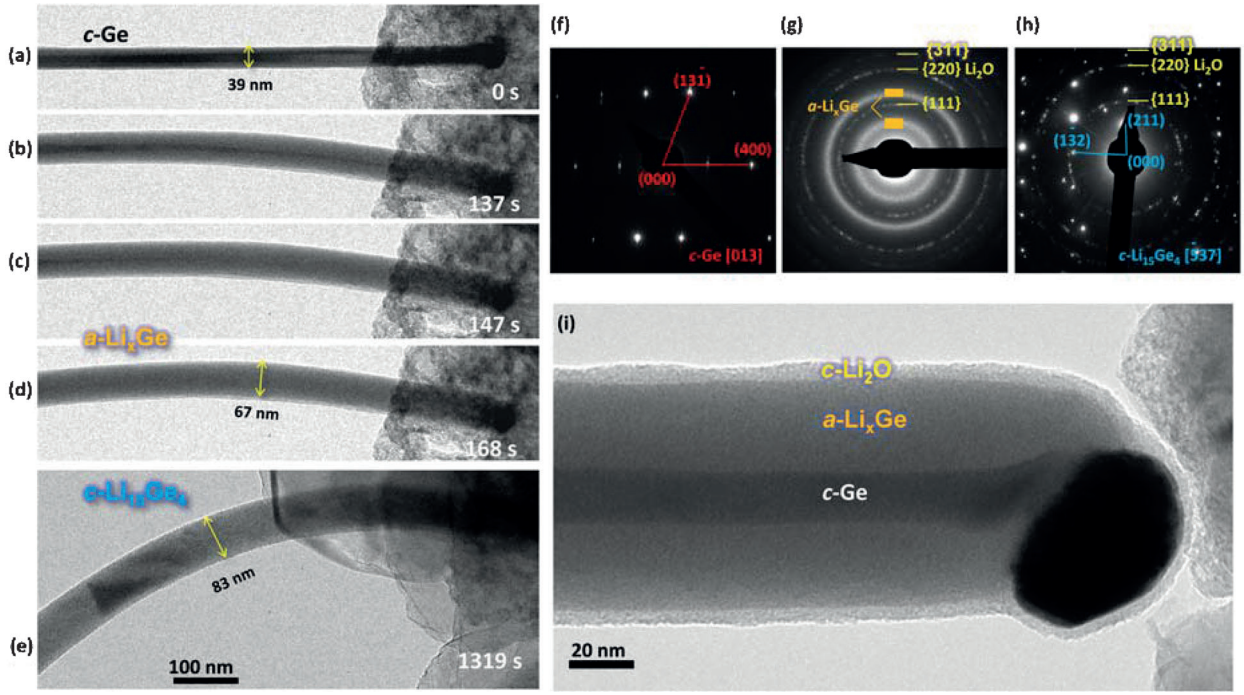

Figure 1. Typical morphology and microstructure evolution in a crystalline Ge nanowire during the first lithiation. The nanowire swelled and elongated upon lithiation (a–d), which converted the crystalline Ge (*c*-Ge) [electron diffraction pattern (EDP) in panel f] into amorphous Li_xGe (*a*-Li_xGe) (EDP in panel g). Subsequently, the *a*-Li_xGe alloy transformed into crystalline $Li_{15}Ge_4$ (*c*-$Li_{15}Ge_4$) (bright TEM image in panel e and EDP in panel h). i) High-magnification TEM image of a zoom-in area of the nanowire during the first lithiation, showing the intermediate state with *c*-Ge core wrapped by *a*-Li_xGe. The surface Li_2O layer is from the lithiation of a native oxide layer on the Ge nanowire surface. Reprinted with permission from ref. [39]. Copyright 2011, American Chemical Society.

fast. The possible phase transformations have been indicated with multiple peaks in the cyclic voltammetry data by Baggetto and Notten.[6] However, further experiments, such as in situ TEM quantitative electrochemistry, are required to correlate the phase changes with the electrochemical signatures. It should be emphasized that the lithiation of *c*-Ge is much faster than that of *c*-Si.[39,79] A complete lithiation of *c*-Ge can be achieved without either high n-type doping or carbon coating. Such difference can be correlated to the fast Li transport in Ge, that is, the Li diffusivity in Ge is about two orders of magnitude higher than that in Si, as extrapolated from high-temperature measurements. On this basis, Ge should be considered as a favorable candidate of the high-rate anode material in LIBs.

The in situ TEM images in Figure 2 show that the lithiated *c*-$Li_{15}Ge_4$ nanowire can be delithiated to amorphous Ge (*a*-Ge) with a nanoporous structure. In ex situ coin cell experiments, a similar porous structure after delithiation was also observed by Cho et al. for Ge nanotubes[13] and by Yuan et al. for Ge nanowires.[12]. The formation of nanopores was attributed to the effective local aggregation of free volumes created during Li extraction, similar to the formation of porous metals in selective dealloying. However, unlike other types of high-capacity electrodes suffering from pulverization during cycling,[46,60] the delithiated porous Ge nanowires neither fractured nor pulverized. Incidentally, we have recently shown the size-dependent fracture of lithiated Si nanomaterials and attributed the tough response of small-sized Si nanoparticles and nanowires to the small fracture driving force (i.e. strain energy release rate), which reduces with decreasing sample size. Such an analysis of the size-dependent fracture driving force should be applicable to Ge nanomaterials.[80] In addition, the fracture resistance of lithiated/delithiated Ge might be higher than that of lithiated/delithiated Si.[40] Further experimental studies of the fracture properties of lithiated/delithiated Ge nanomaterials should be conducted.

In addition, Ge nanowires exhibited a remarkably reversible transformation between *c*-$Li_{15}Ge_4$ and *a*-Ge, as revealed by in situ TEM experiments under multiple cycles (Figure 2). The porous Ge nanowires after each delithiation formed a network structure, retaining the integrity of the Ge electrode which is critical to capacity retention. The porous structure also resulted in an increase of surface area of the electrode to facilitate Li-ion diffusion. During cycling, changes in the outer diameter of the porous Ge nanowire can be reduced, compared to nanowires without a porous structure, because the pores can accommodate most of the volume expansion and contraction. Such an apparent decrease in volume changes can reduce the damages in SEI covering the outer surface of the Ge nanowires. All of these properties promote Ge as a high-rate electrode with less damage accumulation in both the electrode and SEI. Incidentally, to realize the aforementioned advantages, the porous structures are often introduced into high-capacity anode materials during materials synthesis, such as Si,[83,84] Ge,[14,42,85] and GeO_x.[32]

Another interesting feature associated with porous structures is the so-called "pore memory effect" during cycling.[39]

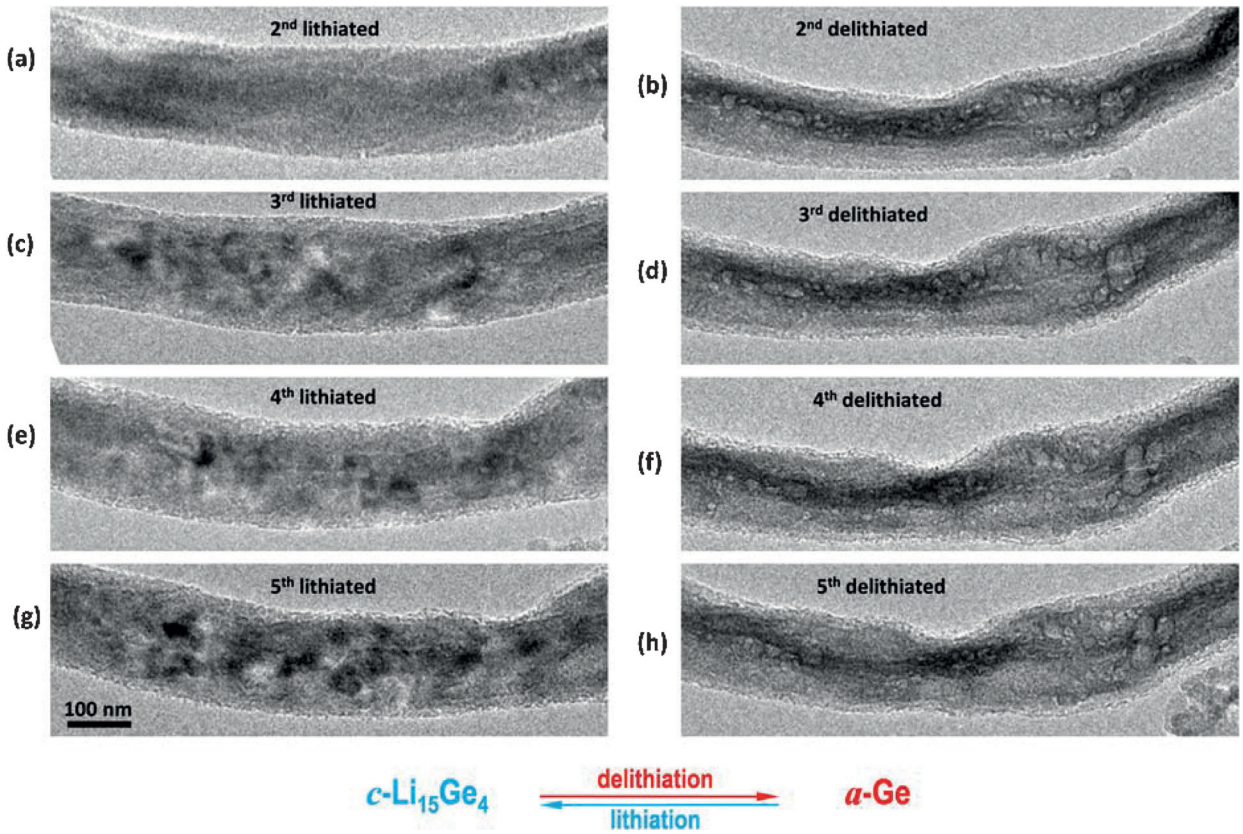

Figure 2. Reversible volumetric changes in four sequential lithiation/delithiation cycles. After each lithiation process, the nanowire became thicker and showed a crystalline contrast (a, c, e, g). After each delithiation process, the nanowire shrunk, became porous, and showed an amorphous contrast (b, d, f, h). The nanowire was transformed between the *c*-$Li_{15}Ge_4$ phase (lithiated) and the *a*-Ge phase (delithiated). The porous structure was only formed at each delithiation stage. Interestingly, the location and distribution of nanopores were almost unchanged. Reprinted with permission from ref. [39]. Copyright 2011, American Chemical Society.

From the second to fifth cycles (shown in Figure 2), it can be seen that the nanopores almost retained their sizes and shapes, and surprisingly reappeared at the same locations during each delithiation (Figures 2 d, f, and h). The "memory" of the porous structure in previous cycles is beneficial for the battery performance because it can minimize the formation of fresh Ge surfaces exposed to electrolytes, thus reducing the formation of extra SEI and increasing the columbic efficiency.

Recently, it has been shown from both in situ[48] and ex situ experiments[86,87] that the lithiation of *c*-Si is highly anisotropic, with the largest and smallest expansion occurring along the $<110>$ and $<111>$ directions, respectively. However, the lithiation of crystalline Ge is almost isotropic, as evidenced by both the axial elongation and radial swelling in $<112>$-Ge nanowires,[39] in contrast with the little axial elongation in $<112>$-Si nanowires.[48] In situ electrochemical experiments under high-resolution TEM imaging have revealed the atomistic origin of the lithiation anisotropy in *c*-Si. It was found that Li ions can hardly penetrate the {111} close-packed Si planes, but can lithiate other crystallographic planes by peeling off the local, inclined, atomic-scale {111} facets via a ledge flow process, as shown in Figures 3 a–b.[88] This orientation dependence of the atomic-scale lithiation underlies the anisotropic swelling in *c*-Si because the slow movement of the reaction front along the $<111>$ directions in *c*-Si significantly delays the expansion along the $<111>$ directions. In contrast, the atomic-scale lithiation process of a $<111>$-Ge nanowire observed from the [110] zone axis shows a different phenomenon (Figure 3 c from our ongoing research). It is worth noting that the crystal geometry of the growth direction as well as the view direction for *c*-Ge (Figure 3 c) is the same as that in the lithiation process of *c*-Si shown in Figure 3 a. The interface between *c*-Ge and *a*-Li_xGe is atomically sharp but the peeling-off effect of each (111) plane was not obvious. This orientation independence of the atomic-scale lithiation can be correlated to the nearly isotropic expansion in *c*-Ge during lithiation, and warrants further study in the future.

Theoretical and computational models have been recently developed to understand the origin of lithiation anisotropy in *c*-Si.[89–94] Based on our early two-phase lithiation model,[48] Yang et al. performed continuum finite element simulations of anisotropic swelling in *c*-Si and showed that lithiation is controlled by the orientation-dependent mobility of the reaction front.[89] Jung et al. employed first-principles molecular dynamics simulations to show that the interfacial energy for the (110) interface is the smallest, which correlates to the preferential expansion along the $<110>$ direction.[90] Chan et al. also conducted first-principles simulations to model the lithiation process in *c*-Si, and showed that the lithiation of a {110} surface is thermodynamically more favorable than that of other surfa-

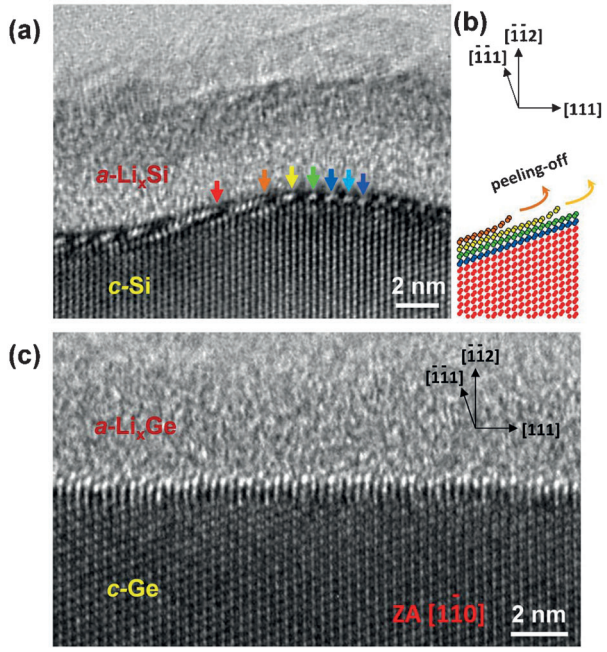

Figure 3. Comparison of the atomic-scale lithiation process between crystalline Si and crystalline Ge. a) High-resolution TEM image showing the lithiation process in crystalline Si through lateral ledge flow at the amorphous-crystalline interface (ACI). b) Schematic representation of peeling-off each layer of the {111} atomic facets in Si. c) High-resolution TEM image showing the lithiation process in crystalline Ge. Note that the growth direction of the nanowires and the viewing direction of the electron beam (zone axis) are the same for Si (a) and Ge (c). The peeling-off process in the lithiation of Ge is not obvious, indicating that the Li ion can easily penetrate the {111} planes in Ge, which can result in the almost isotropic lithiation for Ge, in contrast to the highly anisotropic lithiation for Si. a–b) Reprinted with permission from ref. [88]. Copyright 2012, Nature Publishing Group.

ces.[91] Recently, Cubuk et al. further developed multiscale simulation models to explain the morphological evolution of *c*-Si upon lithiation from a dynamic point of view.[92] However, there are less models for Ge. Chan et al. investigated the onset voltage for lithiation of the (100), (110), and (111) planes in both Si and Ge single crystals by using first-principles calculations, cyclic voltammetry, and Raman spectroscopy. It is found that the onset lithiation voltage of the Si (110) plane is higher than that of the (111) and (100) planes, which is consistent with the experimentally observed preferential expansion along the $<110>$ direction. In contrast, the onset lithiation voltages are close for the above three planes in Ge, indicating the orientation independence of lithiation in Ge.[94] Understanding the physical origin of the difference in lithiation between *c*-Si and *c*-Ge from a kinetic perspective at both the continuum and atomic scales warrants further study.

Another intriguing property of Ge as a promising anode material is its tougher response (compared to Si) during lithiation–delithiation cycling. Lithiation of both *c*-Si and *c*-Ge usually involves a two-phase mechanism, where a sharp interface exists between the crystalline/unlithiated and the amorphous/lithiated phases (Figure 4).[39,48,79,88] Although it has been proven that Si nanostructures exhibit a better cyclability and rate ability compared to their bulk counterparts,[47] there is a critical size for *c*-Si nanoparticles above which fracture always occurs during lithiation.[80] Specifically, individual *c*-Si nanoparticles with different sizes were lithiated during in situ TEM experiments. It was found that Si nanoparticles suffered fracture if the particle size was beyond ~150 nm, and fracture initialized from the surface of the particles. The surface fracture has been attributed to the buildup of a large hoop tension in the outer surface of the Si nanoparticles during two-phase lithiation. Our in situ TEM observation further showed that surface cracking mostly occurs where the adjacent {110} facets intersect. Such a fracture site coincides with the local stress concentration caused by the mismatch of large lithiation expansions normal to the respective {110} facets (Figure 4 g).[80] As shown in Figures 4 a–c, the lithiation in Si is obviously orientation-dependent, as the inner unlithiated core shows a hexagonal shape. In contrast, lithiation in Ge (Figures 4 d–f) is nearly orientation-independent, as evidenced by the nearly uniform thickness of the lithiated shell. The Ge nanoparticles were tough during the lithiation process without any visible cracking. Our continuum chemo-mechanical model further suggested that the tough behavior of Ge could be attributed to the weak anisotropy of lithiation strain at the sharp reaction front.[40]

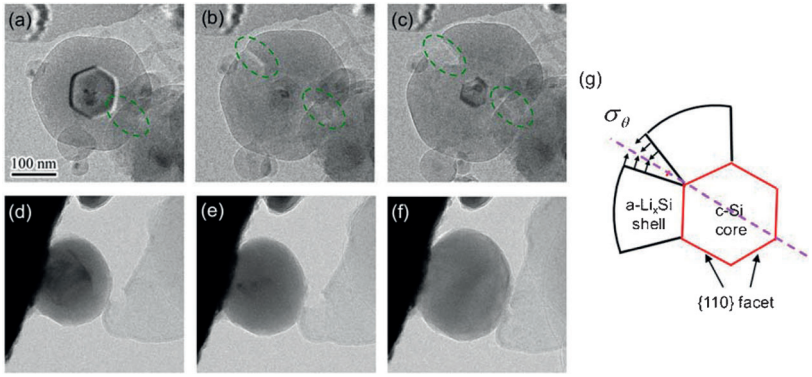

Figure 4. Comparative study of the size-dependent fracture in crystalline Si and the tough behavior in crystalline Ge during lithiation. The original sizes of both Si and Ge nanoparticles are around 160 nm. a–c) Anisotropic swelling and crack formation in a crystalline Si nanoparticle. The partially lithiated particle showed a hexagon-shaped unlithiated Si core with {110} facets. d–f) Nearly isotropic swelling without fracture in a crystalline Ge nanoparticle. g) Schematic showing the development of an intensified hoop tension near the fracture plane (dashed line) due to the anisotropic expansion in crystalline Si. Reprinted with permission from ref. [40]. Copyright 2013, American Chemical Society.

4. Conclusions and Future Research Directions

Building better LIBs is critically important for a number of technological revolutions that scientists and engineers around the world are pursuing. Ge-based electrode materials are promising candidates for the development of high-performance LIBs, owing to the excellent electronic, ionic, and mechanical properties of Ge. In addition to its high capacity, Ge has the advantages of fast lithiation kinetics, formation of memory nanopores, isotropic expansion, and tough response. These combined properties rarely exist in other material systems. Hence, Ge should be considered as a very promising anode material for LIBs. Among a vast list of potentially intriguing directions for future research, several areas present particularly pressing needs:

4.1. Lithiation Mechanism in Amorphous Ge

The lithiation of *a*-Si has been shown to involve a two-step process: *a*-Si $\rightarrow$ *a*-Li_xSi ($x \sim 2.5$) $\rightarrow$ *a*-Li_xSi ($x \sim 3.75$),[81–82] and the first step occurs through a two-phase mechanism, with a sharp interface in between the unlithiated and lithiated parts. A natural question arises: will the lithiation of *a*-Ge also involve the two-step and/or two-phase process? Resolving this question through in situ TEM experiments would provide a fundamental basis for understanding the microstructure evolution, stress generation, and mechanical degradation in *a*-Ge during lithiation.[95] If a sharp interface exists, the novel TEM-based digital image correlation analysis[81] can be applied to map the distribution of lithiation strain, thereby enabling the determination of spatial variation of lithium across the interface. It should be noted that electron diffraction alone might not be sufficient to identify the phases across the interface, since the diffused halos from the amorphous phases would be similar and inaccurate enough to be used for identifying the phases. Quantitative electron energy-loss spectroscopy (EELS) could be employed to distinguish the phases.[96]

4.2. Origin of Isotropic Lithiation in Crystalline Ge

A nearly isotropic swelling has been observed during lithiation of *c*-Ge. However, the atomistic mechanism underlying the isotropic lithiation expansion remains unclear. Ge has the same crystal structure as Si, but the orientation dependence of the lithiation expansion is drastically different in both cases. Understanding the physical basis of this difference may provide guidance for controlling the directionality of lithiation expansion through engineering Si and Ge by alloying. To this end, crucial mechanistic insights could be obtained by in situ TEM imaging of the atomic-scale processes at the phase boundary during lithiation of *c*-Ge.

4.3. Origin of the Tough Behavior of c-Ge

Our TEM studies demonstrated that *c*-Ge nanoparticles reversibly underwent ~260% volume change during multiple lithiation/delithiation cycles without fracture for a large range of sizes from 100 nm to submicrons. While the isotropic expansion could explain the absence of stress concentration at the intersection sites between adjacent {110} facets,[80] it remains unclear why the Ge nanoparticles can survive the large, fast volume expansion without damage and fracture. To address this issue, the aforementioned phase-transformation pathway of Ge needs to be mapped out for its close correlation to the stress generation and evolution. In addition, the mechanical properties and the fracture resistance of the lithiated Ge products need to be carefully measured and modeled as a function of the Li concentration, similar to recent works carried out for Si.[97–99]

4.4. Engineering Ge-Based Electrodes

Given the favorable properties of Ge relative to Si, the performance of Ge-based electrodes could be further improved by coating, processing of Ge-based heterostructures or hybrid structures, and controlling the porosity during cycling. Coatings, such as Al_2O_3 and TiO_2,[100–102] have been applied on the electrode materials to improve the battery performance. Recently, we showed that engineering the coating of Ge nanowires by a conformal, epitaxial, and ultrathin Si surface layer can drastically change the lithiation behavior from the dominant radial lithiation (without coating) to the axial lithiation (with coating).[103] In addition, surface coatings, such as Al_2O_3 and TiO_2, could act as effective protection layers to minimize the consumption of Li during SEI formation, thus increasing the columbic efficiency. Controlling the porosity during cycling is also essential for minimizing the overall volume changes and stabilizing the SEI during cycling.

Acknowledgements

We would like to acknowledge the collaborations with Jian Yu Huang, Xiao Hua Liu, Ju Li, John P. Sullivan, Shadi A. Dayeh, Jinkyoung Yoo, Binh-Minh Nguyen, S. Tom Picraux, Jiangwei Wang, Li Zhong, Scott X. Mao, Sergiy Krylyuk, Albert V. Davydov, Shan Huang, Wentao Liang, Feifei Fan, Hui Yang, Shuman Xia, Hong Li, and Akihiro Kushima. We acknowledge the support by the National Science Foundation under the awards CMMI-1201058 and 1100205. Portions of this work were supported by a Laboratory Directed Research and Development (LDRD) program at Sandia National Laboratories (SNL) and partly by the Nanostructures for Electrical Energy Storage (NEES), an Energy Frontier Research Center (EFRC) funded by the U.S. Department of Energy, Office of Science, Office of Basic Energy Sciences under the Award Number DESC0001160. The LDRD supported the development and fabrication of platforms. The NEES center supported the development of TEM techniques. The Sandia–Los Alamos Center for Integrated Nanotechnologies (CINT) supported the TEM capability. Sandia National Laboratories is a multiprogram laboratory managed and operated by Sandia Corporation, a wholly owned subsidiary of Lockheed Martin Corporation, for the U.S. Department of Energy's National Nuclear Security Administration under Contract DE-AC04-94AL85000.

Keywords: germanium anode · in situ TEM electrochemistry · lithium-ion batteries · nanoporosity · toughness

[1] D. Larcher, S. Beattie, M. Morcrette, K. Edstrom, J.-C. Jumas, J.-M. Tarascon, *J. Mater. Chem.* **2007**, *17*, 3759 – 3772.
[2] C. J. Wen, R. A. Huggins, *J. Solid State Chem.* **1981**, *37*, 271 – 278.
[3] B. A. Boukamp, G. C. Lesh, R. A. Huggins, *J. Electrochem. Soc.* **1981**, *128*, 725 – 729.
[4] M. N. Obrovac, L. Christensen, *Electrochem. Solid-State Lett.* **2004**, *7*, A93 – A96.
[5] M. N. Obrovac, L. J. Krause, *J. Electrochem. Soc.* **2007**, *154*, A103 – A108.
[6] L. Baggetto, P. H. L. Notten, *J. Electrochem. Soc.* **2009**, *156*, A169 – A175.
[7] Y. Kamata, *Mater. Today* **2008**, *11*, 30 – 38.
[8] J. Graetz, C. C. Ahn, R. Yazami, B. Fultz, *J. Electrochem. Soc.* **2004**, *151*, A698 – A702.
[9] C. S. Fuller, J. C. Severiens, *Phys. Rev.* **1954**, *96*, 21 – 24.
[10] C. K. Chan, X. F. Zhang, Y. Cui, *Nano Lett.* **2008**, *8*, 307 – 309.
[11] A. M. Chockla, K. C. Klavetter, C. B. Mullins, B. A. Korgel, *ACS Appl. Mater. Interfaces* **2012**, *4*, 4658 – 4664.
[12] F.-W. Yuan, H.-J. Yang, H.-Y. Tuan, *ACS Nano* **2012**, *6*, 9932 – 9942.
[13] M.-H. Park, Y. Cho, K. Kim, J. Kim, M. Liu, J. Cho, *Angew. Chem.* **2011**, *123*, 9821 – 9824; *Angew. Chem. Int. Ed.* **2011**, *50*, 9647 – 9650.
[14] T. Song, Y. Jeon, M. Samal, H. Han, H. Park, J. Ha, D. K. Yi, J.-M. Choi, H. Chang, Y.-M. Choi, U. Paik, *Energy Environ. Sci.* **2012**, *5*, 9028 – 9033.
[15] K. C. Klavetter, S. M. Wood, Y.-M. Lin, J. L. Snider, N. C. Davy, A. M. Chockla, D. K. Romanovicz, B. A. Korgel, J.-W. Lee, A. Heller, C. B. Mullins, *J. Power Sources* **2013**, *238*, 123 – 136.
[16] B. Laforge, L. Levan-Jodin, R. Salot, A. Billard, *J. Electrochem. Soc.* **2008**, *155*, A181 – A188.
[17] S. Yoon, C.-M. Park, H.-J. Sohn, *Electrochem. Solid-State Lett.* **2008**, *11*, A42 – A45.
[18] M.-H. Seo, M. Park, K. T. Lee, K. Kim, J. Kim, J. Cho, *Energy Environ. Sci.* **2011**, *4*, 425 – 428.
[19] C. H. Kim, H. S. Im, Y. J. Cho, C. S. Jung, D. M. Jang, Y. Myung, H. S. Kim, S. H. Back, Y. R. Lim, C.-W. Lee, J. Park, M. S. Song, W.-I. Cho, *J. Phys. Chem. C* **2012**, *116*, 26190 – 26196.
[20] L. P. Tan, Z. Lu, H. T. Tan, J. Zhu, X. Rui, Q. Yan, H. H. Hng, *J. Power Sources* **2012**, *206*, 253 – 258.
[21] D.-J. Xue, S. Xin, Y. Yan, K.-C. Jiang, Y.-X. Yin, Y.-G. Guo, L.-J. Wan, *J. Am. Chem. Soc.* **2012**, *134*, 2512 – 2515.
[22] K. H. Seng, M.-h. Park, Z. P. Guo, H. K. Liu, J. Cho, *Nano Lett.* **2013**, *13*, 1230 – 1236.
[23] R. A. DiLeo, M. J. Ganter, B. J. Landi, R. P. Raffaelle, *J. Mater. Res.* **2010**, *25*, 1441 – 1446.
[24] R. A. DiLeo, S. Frisco, M. J. Ganter, R. E. Rogers, R. P. Raffaelle, B. J. Landi, *J. Phys. Chem. C* **2011**, *115*, 22609 – 22614.
[25] I.-S. Hwang, J.-C. Kim, S.-D. Seo, S. Lee, J.-H. Lee, D.-W. Kim, *Chem. Commun.* **2012**, *48*, 7061 – 7063.
[26] A. M. Chockla, M. G. Panthani, V. C. Holmberg, C. M. Hessel, D. K. Reid, T. D. Bogart, J. T. Harris, C. B. Mullins, B. A. Korgel, *J. Phys. Chem. C* **2012**, *116*, 11917 – 11923.
[27] J.-G. Ren, Q.-H. Wu, H. Tang, G. Hong, W. Zhang, S.-T. Lee, *J. Mater. Chem. A* **2013**, *1*, 1821 – 1826.
[28] C. Wang, J. Ju, Y. Yang, Y. Tang, J. Lin, Z. Shi, R. P. S. Han, F. Huang, *J. Mater. Chem. A* **2013**, *1*, 8897 – 8902.
[29] S.-H. Woo, S. J. Choi, J.-H. Park, W.-S. Yoon, S. W. Hwang, D. Whang, *J. Electrochem. Soc.* **2013**, *160*, A112 – A116.
[30] J. K. Feng, M. O. Lai, L. Lu, *Electrochim. Acta* **2012**, *62*, 103 – 108.
[31] Y. Kim, H. Hwang, K. Lawler, S. W. Martin, J. Cho, *Electrochim. Acta* **2008**, *53*, 5058 – 5064.
[32] X.-L. Wang, W.-Q. Han, H. Chen, J. Bai, T. A. Tyson, X.-Q. Yu, X.-J. Wang, X.-Q. Yang, *J. Am. Chem. Soc.* **2011**, *133*, 20692 – 20695.
[33] M. G. Kim, J. Cho, *J. Electrochem. Soc.* **2009**, *156*, A277 – A282.
[34] O. B. Chae, S. Park, J. H. Ku, J. H. Ryu, S. M. Oh, *Electrochim. Acta* **2010**, *55*, 2894 – 2900.
[35] C.-M. Hwang, C.-H. Lim, J.-W. Park, *Thin Solid Films* **2011**, *519*, 2332 – 2338.
[36] T. Song, H. Cheng, H. Choi, J.-H. Lee, H. Han, D. H. Lee, D. S. Yoo, M.-S. Kwon, J.-M. Choi, S. G. Doo, H. Chang, J. Xiao, Y. Huang, W. I. Park, Y.-C. Chung, H. Kim, J. A. Rogers, U. Paik, *ACS Nano* **2012**, *6*, 303 – 309.
[37] J. Wang, N. Du, H. Zhang, J. Yu, D. Yang, *J. Mater. Chem.* **2012**, *22*, 1511 – 1515.
[38] C. Yan, W. Xi, W. Si, J. Deng, O. G. Schmidt, *Adv. Mater.* **2013**, *25*, 539 – 544.
[39] X. H. Liu, S. Huang, S. T. Picraux, J. Li, T. Zhu, J. Y. Huang, *Nano Lett.* **2011**, *11*, 3991 – 3997.
[40] W. Liang, H. Yang, F. Fan, Y. Liu, X. H. Liu, J. Y. Huang, T. Zhu, S. Zhang, *ACS Nano* **2013**, *7*, 3427 – 3433.
[41] X. Zhao, C. Wang, D. Wang, H. Hahn, M. Fichtner, *Electrochem. Commun.* **2013**, *35*, 116 – 119.
[42] Y. Yu, C. Yan, L. Gu, X. Lang, K. Tang, L. Zhang, Y. Hou, Z. Wang, M. W. Chen, O. G. Schmidt, J. Maier, *Adv. Energy Mater.* **2013**, *3*, 281 – 285.
[43] Y. Chen, C. Yan, O. G. Schmidt, *Adv. Energy Mater.* **2013**, *3*, 1269 – 1274.
[44] P. R. Abel, A. M. Chockla, Y.-M. Lin, V. C. Holmberg, J. T. Harris, B. A. Korgel, A. Heller, C. B. Mullins, *ACS Nano* **2013**, *7*, 2249 – 2257.
[45] X. H. Liu, Y. Liu, A. Kushima, S. Zhang, T. Zhu, J. Li, J. Y. Huang, *Adv. Energy Mater.* **2012**, *2*, 722 – 741.
[46] L. Y. Beaulieu, K. W. Eberman, R. L. Turner, L. J. Krause, J. R. Dahn, *Electrochem. Solid-State Lett.* **2001**, *4*, A137 – A140.
[47] C. K. Chan, H. Peng, G. Liu, K. McIlwrath, X. F. Zhang, R. A. Huggins, Y. Cui, *Nat. Nanotechnol.* **2008**, *3*, 31 – 35.
[48] X. H. Liu, H. Zheng, L. Zhong, S. Huang, K. Karki, L. Q. Zhang, Y. Liu, A. Kushima, W. T. Liang, J. W. Wang, J.-H. Cho, E. Epstein, S. A. Dayeh, S. T. Picraux, T. Zhu, J. Li, J. P. Sullivan, J. Cumings, C. Wang, S. X. Mao, Z. Z. Ye, S. Zhang, J. Y. Huang, *Nano Lett.* **2011**, *11*, 3312 – 3318.
[49] B. Key, R. Bhattacharyya, M. Morcrette, V. Seznéc, J.-M. Tarascon, C. P. Grey, *J. Am. Chem. Soc.* **2009**, *131*, 9239 – 9249.
[50] P. G. Bruce, B. Scrosati, J.-M. Tarascon, *Angew. Chem.* **2008**, *120*, 2972 – 2989; *Angew. Chem. Int. Ed.* **2008**, *47*, 2930 – 2946.
[51] Y. Wang, H. Li, P. He, E. Hosono, H. Zhou, *Nanoscale* **2010**, *2*, 1294 – 1305.
[52] L. Ji, Z. Lin, M. Alcoutlabi, X. Zhang, *Energy Environ. Sci.* **2011**, *4*, 2682 – 2699.
[53] H. Wu, Y. Cui, *Nano Today* **2012**, *7*, 414 – 429.
[54] K. T. Lee, J. Cho, *Nano Today* **2011**, *6*, 28 – 41.
[55] X. H. Liu, J. Y. Huang, *Energy Environ. Sci.* **2011**, *4*, 3844 – 3860.
[56] J. Y. Huang, L. Zhong, C. M. Wang, J. P. Sullivan, W. Xu, L. Q. Zhang, S. X. Mao, N. S. Hudak, X. H. Liu, A. Subramanian, H. Fan, L. Qi, A. Kushima, J. Li, *Science* **2010**, *330*, 1515 – 1520.
[57] C.-M. Wang, W. Xu, J. Liu, J.-G. Zhang, L. V. Saraf, B. W. Arey, D. Choi, Z.-G. Yang, J. Xiao, S. Thevuthasan, D. R. Baer, *Nano Lett.* **2011**, *11*, 1874 – 1880.
[58] Y. Liu, H. Zheng, X. H. Liu, S. Huang, T. Zhu, J. W. Wang, A. Kushima, N. S. Hudak, X. Huang, S. L. Zhang, S. X. Mao, X. F. Qian, J. Li, J. Y. Huang, *ACS Nano* **2011**, *5*, 7245 – 7253.
[59] A. Kushima, X. H. Liu, G. Zhu, Z. L. Wang, J. Y. Huang, J. Li, *Nano Lett.* **2011**, *11*, 4535 – 4541.
[60] Y. Liu, N. S. Hudak, D. L. Huber, S. J. Limmer, J. P. Sullivan, J. Y. Huang, *Nano Lett.* **2011**, *11*, 4188 – 4194.
[61] H. Ghassemi, M. Au, N. Chen, P. A. Heiden, R. S. Yassar, *ACS Nano* **2011**, *5*, 7805 – 7811.
[62] C.-M. Wang, X. Li, Z. Wang, W. Xu, J. Liu, F. Gao, L. Kovarik, J.-G. Zhang, J. Howe, D. J. Burton, Z. Liu, X. Xiao, S. Thevuthasan, D. R. Baer, *Nano Lett.* **2012**, *12*, 1624 – 1632.
[63] M. Gu, Y. Li, X. Li, S. Hu, X. Zhang, W. Xu, S. Thevuthasan, D. R. Baer, J.-G. Zhang, J. Liu, C. Wang, *ACS Nano* **2012**, *6*, 8439 – 8447.
[64] X. Wang, D.-M. Tang, H. Li, W. Yi, T. Zhai, Y. Bando, D. Golberg, *Chem. Commun.* **2012**, *48*, 4812 – 4814.
[65] M. T. McDowell, I. Ryu, S. W. Lee, C. Wang, W. D. Nix, Y. Cui, *Adv. Mater.* **2012**, *24*, 6034 – 6041.
[66] M. T. McDowell, S. Woo Lee, C. Wang, Y. Cui, *Nano Energy* **2012**, *1*, 401 – 410.
[67] F. Wang, H.-C. Yu, M.-H. Chen, L. Wu, N. Pereira, K. Thornton, A. Van der Ven, Y. Zhu, G. G. Amatucci, J. Graetz, *Nat. Commun.* **2012**, *3*, 1201.
[68] K. Karki, E. Epstein, J.-H. Cho, Z. Jia, T. Li, S. T. Picraux, C. Wang, J. Cumings, *Nano Lett.* **2012**, *12*, 1392 – 1397.
[69] C.-F. Sun, K. Karki, Z. Jia, H. Liao, Y. Zhang, T. Li, Y. Qi, J. Cumings, G. W. Rubloff, Y. Wang, *ACS Nano* **2013**, *7*, 2717 – 2724.

[70] K. E. Gregorczyk, Y. Liu, J. P. Sullivan, G. W. Rubloff, *ACS Nano* **2013**, *7*, 6354 – 6360.
[71] A. Nie, L.-Y. Gan, Y. Cheng, H. Asayesh-Ardakani, Q. Li, C. Dong, R. Tao, F. Mashayek, H.-T. Wang, U. Schwingenschlögl, R. F. Klie, R. S. Yassar, *ACS Nano* **2013**, *7*, 6203 – 6211.
[72] L. Zhong, R. R. Mitchell, Y. Liu, B. M. Gallant, C. V. Thompson, J. Y. Huang, S. X. Mao, Y. Shao-Horn, *Nano Lett.* **2013**, *13*, 2209 – 2214.
[73] Y. Zhu, J. W. Wang, Y. Liu, X. Liu, A. Kushima, Y. Liu, Y. Xu, S. X. Mao, J. Li, C. Wang, J. Y. Huang, *Adv. Mater.* **2013**, *25*, 5461 – 5466.
[74] Q. Su, L. Chang, J. Zhang, G. Du, B. Xu, *J. Phys. Chem. C* **2013**, *117*, 4292 – 4298.
[75] Q. Su, Z. Dong, J. Zhang, G. Du, B. Xu, *Nanotechnology* **2013**, *24*, 255705.
[76] M. Gu, Z. Wang, J. G. Connell, D. E. Perea, L. J. Lauhon, F. Gao, C. Wang, *ACS Nano* **2013**, *7*, 6303 – 6309.
[77] P. Limthongkul, *J. Power Sources* **2003**, *119 – 121*, 604 – 609.
[78] P. Limthongkul, Y.-I. Jang, N. J. Dudney, Y.-M. Chiang, *Acta Mater.* **2003**, *51*, 1103 – 1113.
[79] X. H. Liu, L. Q. Zhang, L. Zhong, Y. Liu, H. Zheng, J. W. Wang, J.-H. Cho, S. A. Dayeh, S. T. Picraux, J. P. Sullivan, S. X. Mao, Z. Z. Ye, J. Y. Huang, *Nano Lett.* **2011**, *11*, 2251 – 2258.
[80] X. H. Liu, L. Zhong, S. Huang, S. X. Mao, T. Zhu, J. Y. Huang, *ACS Nano* **2012**, *6*, 1522 – 1531.
[81] J. W. Wang, Y. He, F. Fan, X. H. Liu, S. Xia, Y. Liu, C. T. Harris, H. Li, J. Y. Huang, S. X. Mao, T. Zhu, *Nano Lett.* **2013**, *13*, 709 – 715.
[82] M. T. McDowell, S. W. Lee, J. T. Harris, B. A. Korgel, C. Wang, W. D. Nix, Y. Cui, *Nano Lett.* **2013**, *13*, 758 – 764.
[83] H. Kim, B. Han, J. Choo, J. Cho, *Angew. Chem.* **2008**, *120*, 10305 – 10308; *Angew. Chem. Int. Ed.* **2008**, *47*, 10151 – 10154.
[84] M. Ge, J. Rong, X. Fang, C. Zhou, *Nano Lett.* **2012**, *12*, 2318 – 2323.
[85] L. C. Yang, Q. S. Gao, L. Li, Y. Tang, Y. P. Wu, *Electrochem. Commun.* **2010**, *12*, 418 – 421.
[86] J. L. Goldman, B. R. Long, A. A. Gewirth, R. G. Nuzzo, *Adv. Funct. Mater.* **2011**, *21*, 2412 – 2422.
[87] S. W. Lee, M. T. McDowell, J. W. Choi, Y. Cui, *Nano Lett.* **2011**, *11*, 3034 – 3039.
[88] X. H. Liu, J. W. Wang, S. Huang, F. Fan, X. Huang, Y. Liu, S. Krylyuk, J. Yoo, S. A. Dayeh, A. V. Davydov, S. X. Mao, S. T. Picraux, S. Zhang, J. Li, T. Zhu, J. Y. Huang, *Nat. Nanotechnol.* **2012**, *7*, 749 – 756.
[89] H. Yang, S. Huang, X. Huang, F. Fan, W. Liang, X. H. Liu, L.-Q. Chen, J. Y. Huang, J. Li, T. Zhu, S. Zhang, *Nano Lett.* **2012**, *12*, 1953 – 1958.
[90] S. C. Jung, J. W. Choi, Y.-K. Han, *Nano Lett.* **2012**, *12*, 5342 – 5347.
[91] M. K. Y. Chan, C. Wolverton, J. P. Greeley, *J. Am. Chem. Soc.* **2012**, *134*, 14362 – 14374.
[92] E. D. Cubuk, W. L. Wang, K. Zhao, J. J. Vlassak, Z. Suo, E. Kaxiras, *Nano Lett.* **2013**, *13*, 2011 – 2015.
[93] M. Pharr, K. Zhao, X. Wang, Z. Suo, J. J. Vlassak, *Nano Lett.* **2012**, *12*, 5039 – 5047.
[94] M. K. Y. Chan, B. R. Long, A. A. Gewirth, J. P. Greeley, *The Journal of Physical Chemistry Letters* **2011**, *2*, 3092 – 3095.
[95] S. Huang, F. Fan, J. Li, S. L. Zhang, T. Zhu, *Acta Mater.* **2013**, *61*, 4354 – 4364.
[96] J. Danet, T. Brousse, K. Rasim, D. Guyomard, P. Moreau, *PCCP* **2010**, *12*, 220 – 226.
[97] B. Hertzberg, J. Benson, G. Yushin, *Electrochem. Commun.* **2011**, *13*, 818 – 821.
[98] F. Feifei, H. Shan, Y. Hui, R. Muralikrishna, D. Dibakar, B. S. Vivek, C. T. v. D. Adri, Z. Sulin, Z. Ting, *Modell. Simul. Mater. Sci. Eng.* **2013**, *21*, 074002.
[99] M. Pharr, Z. Suo, J. J. Vlassak, *Nano Lett.* **2013**, *13*, 5570 – 5577.
[100] X. Xiao, P. Lu, D. Ahn, *Adv. Mater.* **2011**, *23*, 3911 – 3915.
[101] E. Memarzadeh Lotfabad, P. Kalisvaart, K. Cui, A. Kohandehghan, M. Kupsta, B. Olsen, D. Mitlin, *PCCP* **2013**, *15*, 13646 – 13657.
[102] X. Meng, X.-Q. Yang, X. Sun, *Adv. Mater.* **2012**, *24*, 3589 – 3615.
[103] Y. Liu, X. H. Liu, B.-M. Nguyen, J. Yoo, J. P. Sullivan, S. T. Picraux, J. Y. Huang, S. A. Dayeh, *Nano Lett.* **2013**, *13*, 4876 – 4883.

Received: October 18, 2013
Revised: December 12, 2013
Published online on January 30, 2014